*Semiconductors, 2024, Vol. 58, No. 12*

# Evolution of composition and topography of $A^{III}B^{V}$ semiconductors during sputtering with argon ions

© *A.E. Ieshkin*[1], *A.A. Tatarintsev*[1], *B.R. Senatulin*[2], *E.A. Skryleva*[2]

[1] Department of Physics, Moscow State University,
119991 Moscow, Russia
[2] National University of Science and Technology MISiS,
119049 Moscow, Russia
E-mail: ieshkin@physics.msu.ru

*Received November 13, 2024*
*Revised January 15, 2025*
*Accepted January 15, 2025*

A systematic study of the composition and structure of the surface of $A^{III}B^{V}$ semiconductors (GaP, GaAs, GaSb, InP, InAs, InSb) after irradiation with 3 keV argon ions was carried out. The surface composition was determined using X-ray photoelectron spectroscopy. The results obtained are discussed in terms of preferential sputtering and radiation-stimulated segregation. It is shown that the observed enrichment with the metallic component is not explained by these processes alone. A developed relief in the form of nanopillars was observed on the surface of indium-containing materials, while no relief development was found on the GaP surface. This behavior is associated with the patterns of wetting of the semiconductor surface by the surface-enriching component.

**Keywords:** sputtering, $A^{III}B^{V}$, nanotopography, preferential sputtering, surface segregation, XPS.

DOI: 10.61011/SC.2024.12.60385.7328

## 1. Introduction

Semiconductor materials of the $A^{III}B^{V}$ group have become the basis for creating light-emitting and detecting structures, microelectronics devices, solar energy in a wide spectral range [1]. Accelerated ion beams occupy one of the central places in the physics and technology of semiconductors in the modification of the surface layers (ion doping [2], surface cleaning [3]) and their analysis (Rutherford backscattering and secondary ion mass spectrometry techniques, ion profiling in X-ray photoelectron spectroscopy — XPS).

Exposure of a crystal surface to an ion beam leads to a whole set of processes such as creation of radiation damage, implantation and adsorption of impurities, and sputtering [4]. In the case of multicomponent materials, these processes are supplemented by preferential sputtering of one of the components, radiation-enhanced diffusion and segregation [5]. As a result, a layer with altered structure, composition, and topography appears near the surface.

The effect of ion irradiation (primarily noble gas ions) on the surface of semiconductors of the $A^{III}B^{V}$ group has been investigated for a long time. Thus, in the 80's and 90's of the XX century a large number of works were devoted to elucidation of the composition of the modified surface layer and the mechanisms of formation of this layer. These results are summarized in an extensive overview [6,7]. Note that most of these works do not discuss the formation of nanorelief on the irradiated surface, which often leads to a misunderstanding of the processes involved. Nanorelief and nanostructures arising on the surface of such semiconductors as a result of ion bombardment, have been widely studied only in the XXI century. One of the impetus for this was the discovery of self-forming under the influence of ion irradiation ordered relief on the surface of GaSb [8]. Often the studies of relief formation were not accompanied by a direct study of the surface composition, despite the fact that the modern understanding of the mechanism of the origin of such relief is based on the chemical instability of the layer with the composition changed by ion irradiation [9,10]. Thus, despite their large number, studies of ion modification of the composition and structure of $A^{III}B^{V}$ semiconductors are rather scattered, conducted under different conditions, and often important irradiation parameters, such as ion fluence and density current, are not specified.

In this paper, we investigated the dynamics of the composition of the near-surface layer during ion irradiation under ultrahigh vacuum conditions for a wide range of materials (GaP, GaAs, GaSb, InP, InAs, InSb) and described the relief formed on the surface. The experiments were carried out at fixed ion beam parameters, which allows direct comparison.

## 2. Experiment procedure

Ion irradiation and surface composition analysis of single-crystal wafers were performed on a PHI 5000 VersaProbeII (ULVAC-PHI). An ion gun was used for irradiation, forming a beam of argon ions with an energy of 3 keV and a current $3-3.5\,\mu$A. For samples containing antimony, the ion energy was reduced to 2 keV to ensure that the penetration depth was close to the other samples. In the case of GaP and GaAs, additional measurements were performed with an ion energy of 0.5 keV and a current $0.75-0.85\,\mu$A. The

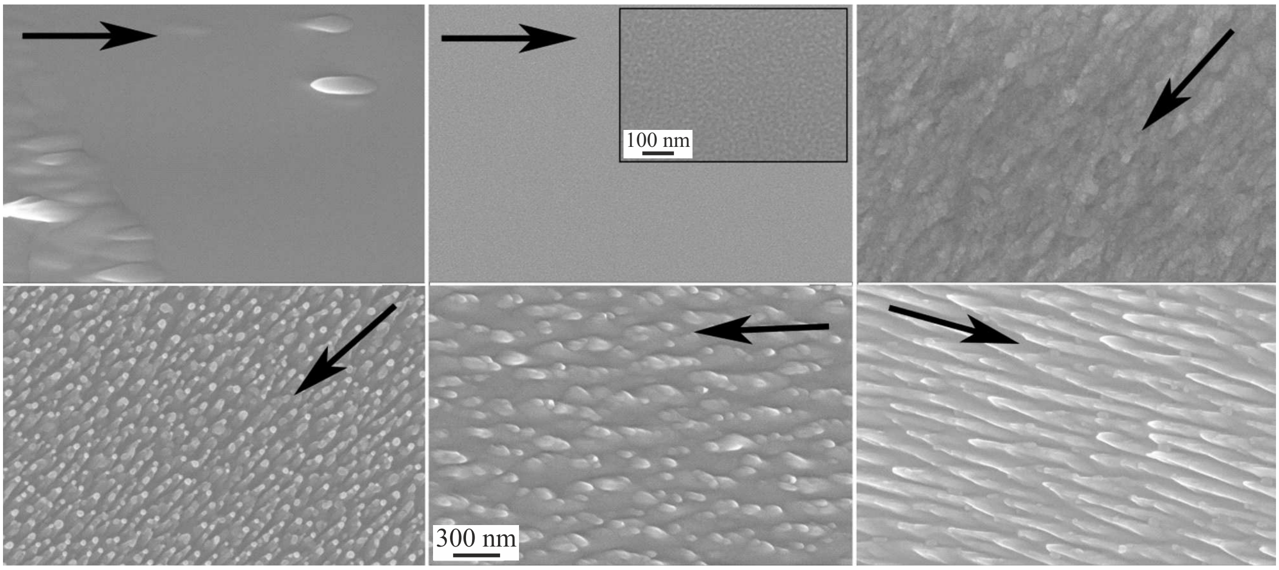

**Figure 1.** SEM images of the semiconductor surface after ion etching: top row from left to right — GaP, GaAs, GaSb, bottom row — InP, InAs, InSb.

**Table 1.** The penetration depth and straggling of argon ions at the angle of incidence 55° according to TRIM [11] and the photoelectron inelastic mean free path (IMFP) for the angle 45° according to QUASES [12]

| | Penetration depth, Å | | IMFP · cos 45°, Å | |
|---|---|---|---|---|
| GaP | $36 \pm 23$ | (3 keV) | Ga $3p$ | 20 |
| | $13 \pm 8$ | (0.5 keV) | P $2s$ | 19 |
| GaAs | $36 \pm 23$ | (3 keV) | Ga $3p$ | 20 |
| | $14 \pm 9$ | (0.5 keV) | As $3d$ 30 | 21 |
| GaSb | $36 \pm 24$ | (2 keV) | Ga $3d$ 32 | 22 |
| | | | Sb $4d$ 32 | 22 |
| InP | $44 \pm 29$ | (3 keV) | In $3d_{5/2}$ | 17 |
| | | | P $2s$ 28 | 20 |
| InAs | $45 \pm 29$ | (3 keV) | In $3d_{5/2}$ | 17 |
| | | | As $3d$ 28.5 | 22 |
| InSb | $42 \pm 27$ | (2 keV) | In $4d$ | 24 |
| | | | Sb $4d$ | 24 |

beam incidence direction was 55° from the normal to the sample surface. The depth of ion penetration under these conditions is given in Table 1. The beam was scanned within the region $2 \times 3.5$ mm on the sample surface. In the center of this region, the composition was analyzed by XPS. During the experiment, cycles of ion etching and analysis were alternated, which allowed us to observe the dynamics of the surface composition.

X-ray photoelectrons were excited by monochromatized Al$K_\alpha$, radiation focused into a region with a diameter of 0.2 mm. The analyzer axis was directed at an angle 45° from the normal to the sample, the angle between the planes of incidence of the ion beam and the plane of analysis 90°. Analytical lines were chosen so that the photoelectron inelastic mean free path was close for all elements (Table 1). Prior to the experiment, semiconductor wafers from orientation (001) were cleaved so that (001) surface was exposed to ion irradiation. The relative elemental sensitivity factors PHI, used to calculate the atomic concentrations of elements from the photoelectron line intensities, were corrected on the cleaved wafers, checking that the content of oxidized components on the cleavage did not exceed a few percent, i. e., selective oxidation and segregation did not introduce noticeable distortions. After the steady-state surface composition was reached, composition determination was carried out for a long time without accompanying etching to determine the concentration measurement error.

The pressure in the chamber before the experiment was $\leq 3 \cdot 10^{-8}$ Pa.

The surface topography of the samples after ion irradiation was examined using a Zeiss Ultra 55 scanning electron microscope (SEM).

## 3. Results and discussion

### 3.1. Surface topography

Figure 1 shows the images of the semiconductor surface after sputtering by ions with energy of 3 keV in the SEM. In case of GaP, the surface remained smooth (a small region containing surface defects is shown). On the GaAs surface a weakly pronounced chaotic relief is observed, noticeable only at maximum magnification. On GaSb the relief is more pronounced, having orientation along the direction of ion beam propagation.

On the surface of all semiconductors containing indium, after ion irradiation a relief in the form of pillars oriented towards the ion beam appeared. This type of relief developing on two-component semiconductors is well known both for the group $A^{III}V^{V}$ [13,14], and for other types [15,16] and appears in a wide range of ion energies — from hundreds of eV [15] to 50−100 keV and more [17]. The structure of the pillars can be seen in particular detail on InP. It can be seen that there is a lighter colored bead at the top. It is known from literature that it consists of a metallic component, while the composition of the pillar corresponds to a bulk material.

The mechanism for the appearance of this relief is now attributed to chemical instability occurring in the near-surface layers. As will be shown below (Figures 2, 3), during ion sputtering, the near-surface layers are enriched with a metallic component (Ga or In). At a sufficient degree of enrichment near the surface, phase separation occurs with the separation of metallic nuclei. During further sputtering they serve as a mask under which pillars appear. The metal islands are fed by ion-stimulated diffusion along the surface, which allows them to persist during the sputtering process. Note that the further growth of pillars can be associated not only with shadowing, but also with the re-deposition of sputtered material (both components of the target) and its further release from the metal island into the pillar volume (vapor-liquid-solid mechanism) [15].

The absence of relief on the surface of GaP and GaAs and its presence on GaSb in [10] is explained by the difference in thermodynamic properties of the materials. In this paper it is assumed that the energy density released as a result of the ion impact on the target is sufficient to cause local melting and an increase in the mobility of atoms, contributing to the development of chemical instability. The molten region has the smallest volume for GaP and the largest for GaSb, which explains the least pronounced relief in the former case and it is the most pronounced — in the latter. However, to be able to talk about thermal conductivity and melting, the collision cascade must be highly nonlinear, i. e., a large number of atoms (compared to their total number) within the cascade volume must be in motion. According to TRIM data, an argon ion with an energy of 3 keV has an elastic energy loss in GaAs of 42 eV/Å and creates on average 75 vacancies, while the total number of atoms in the volume occupied by the cascade is several thousand (with longitudinal and radial straggling of 24 and 22 Å respectively) Thus, it is difficult to speak of a nonlinear cascade (although it may be noted that in other works this concept was also attracted to explain the porous structure of complex semiconductors in some modes of ion irradiation [18], on the other hand, porous layer due to the accumulation of gas under the surface, was found in [19] in the irradiation of gallium arsenide light neon ions). In addition, when irradiated with bismuth ions with an energy of 10 keV (i. e., at significantly higher energy release and the degree of nonlinearity of the cascade), the relief was also not detected on GaP and weakly manifested on GaAs. We present for comparison the estimation of the parameters of such a cascade using TRIM. The elastic energy loss of the bismuth ion with an energy of 10 keV in GaAs is 202 kV/Å, the number of vacancies created is 270 at longitudinal and radial straggling of 24 and 16 Å respectively (at normal incidence).

Therefore, the absence of relief on GaP must be explained by other reasons. The formation of metal islands at the initial stage of nanopillars growth can be described as the formation of a metal film on the semiconductor surface. It is known that depending on the ratio of the bond energy of the film atoms to each other and to the substrate, different growth mechanisms are possible — island growth (Volmer-Weber) or layer-by-layer Frank–van der Merwe growth mode. It can be assumed that in the case of GaP, the gallium atoms enriching the surface during sputtering remain bound to the surface and the film does not tend to split into islands as in the case of other semiconductors. This is confirmed by the highest dissociation energy of the GaP molecule (2.38 eV, [20]) compared to molecules of other substances used — about 2 eV (1.57 eV for InSb).

### 3.2. Surface composition

Let us now consider the evolution of the surface composition during the sputtering process. For gallium-containing materials it is shown in Figure 2. The thickness of the removed layer was estimated using sputtering yields from TRIM simulation data. This estimation does not take into account the surface topography, which can significantly change the sputtering coefficient, so the indicated thicknesses are rather approximate. Similar dependences were obtained for indium-containing materials.

The establishment of the equilibrium composition occurs already at the first sputtering cycles and corresponds to the etching depth ∼ 10 nm. It is known that at such fluences on the surface of some of the used materials (as will be discussed below) relief in the form of metallic islands begins to form, which develop into a system of pillars with increasing fluence. Interestingly, at the stage of pillar development, the measured surface composition no longer changes. In accordance with the geometry of the experiment, the photoelectron detector is directed to the sides of the pillars (in the plane perpendicular to the plane of beam incidence and pillar growth).

According to current perception, several mechanisms play a role in establishing the composition of the near-surface layers. One of them — preferential sputtering of one of the components. It is believed that the component with lower surface bond energy $U$ and lower atomic mass $M$ should preferentially be sputtered. In the approximation of an unchanged target (i. e., low dose), Sigmund derived the formula [21]

$$\frac{C_s^{\mathrm{A}}}{C_s^{\mathrm{B}}} = \left(\frac{C_{\mathrm{A}}}{C_{\mathrm{B}}}\right)\left(\frac{M_{\mathrm{A}}}{M_{\mathrm{B}}}\right)^{2m}\left(\frac{U_s^{\mathrm{A}}}{U_s^{\mathrm{B}}}\right)^{1-2m}, \quad (1)$$

where $m$ — coefficient, at low ion energies (of the order of keV) taking values from 0 to 0.2, $C_{\mathrm{A}}$ and $C_s^{\mathrm{A}}$ —

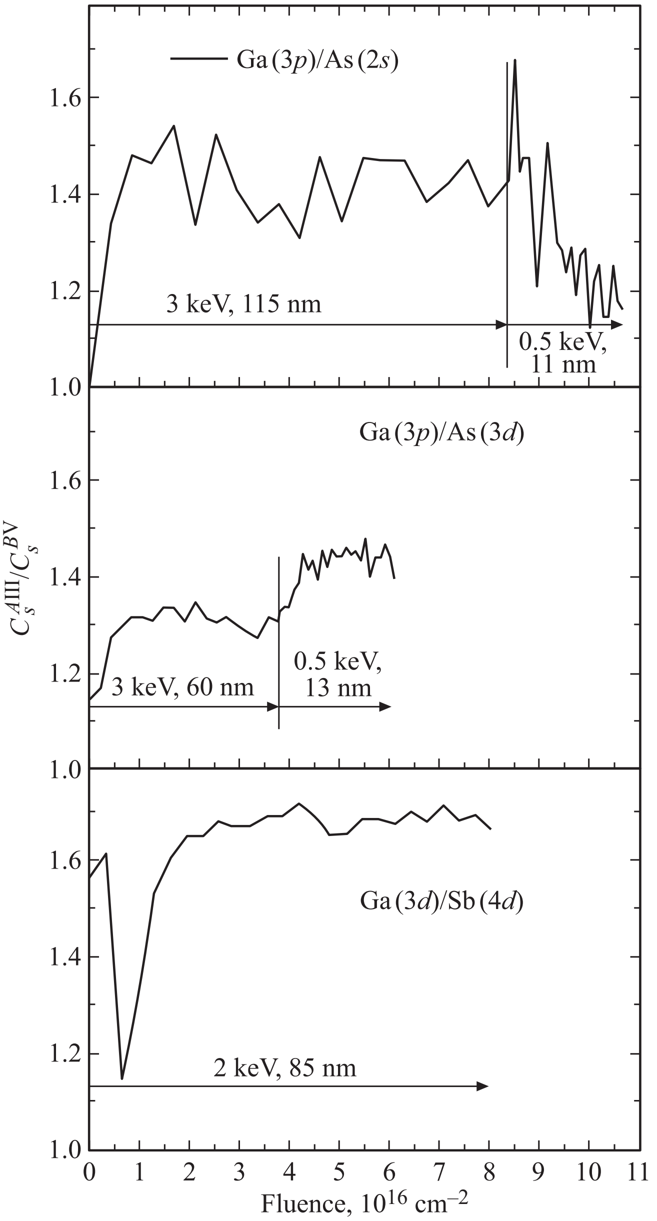

**Figure 2.** Dose dependences of the atomic concentration ratios of the components in the surface layer.

bulk and surface concentrations of component A. In our calculations we used the value $2m = 0.33$ [7]. In this case, since the yield depth of sputtered atoms is $\sim 2$ monolayers, preferential sputtering means that in the steady state, the $C_s^{\mathrm{A}}$ in Sigmund's formula refers to the composition of these very layers. Another mechanism affecting the surface composition, — radiation-stimulated segregation, which tends to minimize the free energy of the top layer. Most often, segregation results in the surface being enriched (compared to the second atomic layer) with a component with a lower binding energy. The composition of deeper layers (up to maximum depth of ion penetration) is established as a result of ion-stimulated diffusion.

**Table 2.** Characteristics of chemical elements [24]

| Element | Atomic number | Atomic mass (a.e.m.) | Bond energy on the surface, eV |
|---|---|---|---|
| Ga | 31 | 69.7 | 2.82 |
| In | 49 | 114.8 | 2.49 |
| P | 15 | 31 | 3.28 |
| As | 33 | 74.9 | 2.98 |
| Sb | 51 | 121.8 | 2.72 |
| Ar | 18 | 40 | |

It should be noted that the exact values of the bond energy of an atom on the surface are currently unknown. For pure substances, it is identified with the enthalpy of sublimation. For multicomponent materials, this value must depend on the surface composition, and there are several approaches to its description [22,23]. The enthalpy of sublimation of pure substances was also used to estimate from the formula (1) (Table 2). Data on the enthalpy of sublimation of arsenic in the literature differ. In accordance with [24], the value for gray arsenic — 3.14 eV (used, for example, in [25]), for yellow arsenic — 2.98 eV. The value used in the TRIM database is 1.26 eV. In our calculations, we used the value of 2.98 eV used by Sich, which provided a good match for the GaAs [25] sputtering coefficient. Note that in [25,26] segregation of arsenic on the surface of GaAs and InAs was noted, i. e., the value of the bond energy of arsenic on the surface may be less than this value.

The surface composition in the steady state, determined from the XPS data, and the results of estimation by the formula (1) are shown in Figure 3. The near-surface layers of all materials are enriched with gallium or indium. We

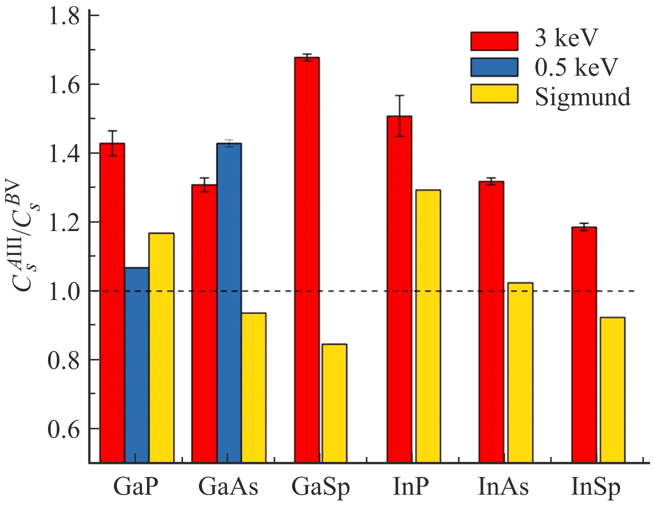

**Figure 3.** The ratios of the component concentrations in the surface layer (based on XPS data) after the steady state is reached. Experimental data from sputtering at energies of 3 and 0.5 keV and calculation by formula (1). (A color version of the figure is provided in the online version of the paper).

emphasize that the XPS technique provides information on the averaged composition of a layer with a thickness of the order of the photoelectron yield depth (Table 1). Qualitatively, the formula (1) in the GaP−GaSb and InP−InSb series gives a trend similar to the experimental one, except for GaSb. This exception may be due to the fact that the surface bond energy of antimony atom is smaller than that of gallium atom. Segregation of antimony to the surface with subsequent sputtering of the segregated atoms occurs, resulting in significant gallium enrichment. A similar result was observed in the sputtering of NiTi alloy, for which the evaluation predicted titanium enrichment, but nickel enrichment was observed, which was explained by chemical segregation of titanium to the surface [27].

Despite the qualitative agreement of the trend obtained from formula (1) with experiment, quantitatively this estimate does not coincide with the experimental results. Moreover, in some cases it predicts gallium or indium depletion, which is not observed. Segregation also cannot explain the result obtained. For example, in the case of InSb, indium enrichment is observed. However, indium should sputter preferentially (in accordance with Sigmund's formula) and at the same time segregate to the surface (due to lower bond energy), i. e., segregation should further enhance the subsurface indium depletion. The preferential sputtering in Sigmund's description, as well as the consideration of segregation, implies homogeneity of the target in the lateral direction. Therefore, it can be assumed that the formation of the surface composition is due to the three-dimensional dynamics of the local composition of the near-surface layers at the initial stage of irradiation. The formation of defect clusters and phase separation in the lateral direction leads to the development of the surface topography, which in turn affects the further evolution of the composition [28].

The formula (1) does not include the ion beam energy. Experimentally, the dependence of the enrichment value on energy has been observed in a number of cases, but such results are rather inconsistent [7]. One reason why ion energy may influence the observed surface composition, — the relationship between the thickness of the modified layer (near the depth of ion penetration) and the information layer in the measurement method used. In some cases, non-monotonic time dependencies of component concentration were observed with changing ion beam energy [29].

Figure 4 qualitatively shows a theoretical approximate character of the profile of component concentration in the presence of preferential sputtering and segregation, as well as an approximate scale of the information depth of the XPS lines used. To plot such a profile, TRIM data on the depth of ion penetration, which determines the thickness of the altered composition layer, were used. The composition of the upper atomic layers is determined by preferential sputtering so that the composition of the sputtered material coincides with the bulk composition. If a component B is preferentially sputtered, the surface is enriched with a second component A. Therefore, the surface composition was fixed at some level determined by the degree of preferential sputtering. Further, since the component segregating to the surface enriches the upper atomic layer compared to the second layer, depending on the segregation direction, the subsurface composition approaches or moves away from the bulk composition, which was also shown in Figure 4. The degree of enrichment of deeper layers is determined by the rate of segregation and radiation-induced diffusion. If the depth of ion penetration is sufficiently small compared to the depth of photoelectron yield, the observed decrease in the degree of enrichment occurs.

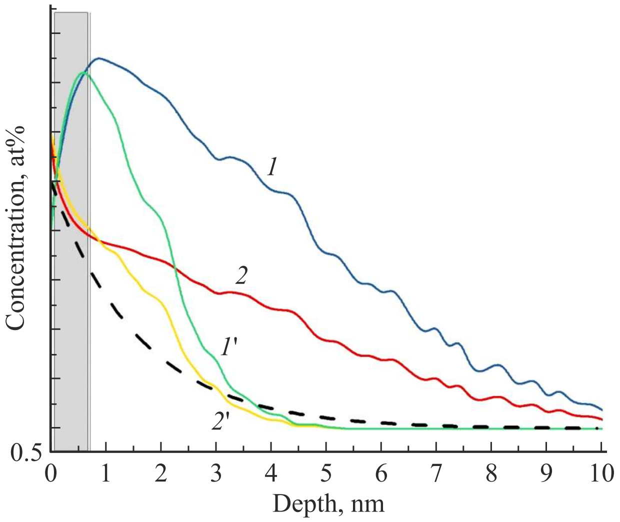

**Figure 4.** View of the concentration profile of a component that is not preferentially sputtered when sputtered with ions of energy 3 keV (curves *1, 2*) and 0.5 keV (1′, 2′). As the result of segregation, the surface is enriched (1, 1′) or depleted 2, 2′) by the preferentially sputtered component. The dotted line shows the photoelectron emission probability. The segregation region is highlighted in gray.

In case of GaP and GaAs, which did not develop significant relief on the surface, two ion beam energies were used successively. For GaP, the transition from an energy of 3 keV to an energy of 0.5 keV resulted in a surface composition close to the bulk composition. By contrast, in case of GaAs, the surface enrichment of gallium monotonically increased. This difference may be due to the fact that there was no relief on the GaP surface, and the concentration of excess gallium monotonically decreased with depth at both 3 keV and 0.5 keV energies. On the GaAs surface, some relief was still observed, i. e., the component concentration along the surface also changed during the transition to a different energy.

## 4. Conclusion

Thus, at irradiation of semiconductor compounds AIII$B^{V}$ there was enrichment of the surface with indium or gallium. After reaching the equilibrium value (at fluence $\sim 10^{16}\,\mathrm{cm}^{-2}$) the measured composition value did not change despite the development of pronounced relief for most compounds. The observed enrichment is quantitatively inconsistent with the evaluation by the Sigmund formula. In case of GaSb, this difference can be explained by segregation of antimony and its subsequent sputtering, which does not explain the differences for other materials. Thus, it can be assumed that the formation of the surface composition of the considered compounds is associated with the three-dimensional dynamics of the local composition of the near-surface layers. The formation of defect clusters and phase separation in the lateral direction leads to the development of the surface topography, which in turn affects the further evolution of the composition. Thus, a self-consistent three-dimensional consideration of composition and surface topography is necessary to develop models of compound modification by ion irradiation.

The absence of relief on GaP after ion irradiation can be attributed to the continuous nature of the film (modified layer) on the surface. In case of GaAs, the relief was weakly pronounced, while developed structures in the form of pillars with metal tops oriented toward the ion beam were observed on indium-containing compounds.

### Conflict of interest

The authors declare that they have no conflict of interest.

## References

[1] M.P. Mikhailova, K.D. Moiseev, Y.P. Yakovlev. Semiconductors, **53**, 273 (2019). DOI: 10.1134/S1063782619030126)

[2] A.I. Struchkov, K.V. Karabeshkin, P.A. Karasev, A.I. Titov. FTP, **57** (9), 738 (2023). (in Russian). DOI: 10.61011/SC.2024.12.60385.7328

[3] A.S. Tokarev, O.A. Lapshina, A.A. Kozyrev. Semiconductors, **57** (1), 54 (2023). DOI: 10.61011/SC.2024.12.60385.7328)

[4] B. Rauschenbach. *Low-Energy Ion Irradiation of Materials. Fundamentals and Application* (Springer, 2022). DOI: 10.1007/978-3-030-97277-6

[5] N.Q. Lam, H. Wiedersich. Methods B, **18**, 471 (1986). DOI: 10.1016/S0168-583X (86)80073-8

[6] J.B. Malherbe. Crit. Rev. Solid State Mater. Sci., **19** (2), 55 (1994). DOI: 10.1080/10408439408244588

[7] J.B. Malherbe. Crit. Rev. Solid State Mater. Sci., **19** (3), 129 (1994). DOI: 10.1080/10408439408244589

[8] S. Facsko, T. Dekorsy, C. Koerdt, C. Trappe, H. Kurz, A. Vogt, H.L. Hartnagel. Science, **285**, 1551 (1999). DOI: 10.1126/science.285.5433.1551

[9] S. Le Roy, E. Barthel, N. Brun, A. Lelarge, E. Søndergård. J. Appl. Phys., **106**, 094308 (2009). DOI: 10.1063/1.3243333

[10] O. El-Atwani, S.A. Norris, K. Ludwig, S. Gonderman, J.P. Allain. Sci. Rep., **5**, 18207 (2015). DOI: 10.1038/srep18207

[11] www.srim.org

[12] www.quases.com/products/quases-imfp-tpp2m

[13] T.K. Chini, J. Kato, M. Tanemura, F. Okuyama. Methods B, **95**, 313 (1995). DOI: 10.1016/0168-583X (94)00539-7

[14] E. Trynkiewicz, B.R. Jany, D. Wrana, F. Krok. Appl. Surf. Sci., **427**, 349 (2018). DOI: 10.1016/j.apsusc.2017.08.240

[15] S.P. Zimin, I.I. Amirov, M.S. Tivanov, N.N. Kolesnikov, O.V. Korolik, L.S. Lyashenko, D.V. Zhyhulin, L.A. Mazaletskiy, S.V. Vasilev, O.V. Savenko. Phys. Solid State, **65** (4), 671 (2023). DOI: 10.61011/SC.2024.12.60385.7328

[16] S.P. Zimin, N.N. Kolesnikov, I.I. Amirov, V.V. Naumov, E.S. Gorlachev, S. Kim, N.H. Kim. Crystals, **12**, 111 (2022). DOI: 10.3390/cryst12010111

[17] I. Sulania, P. Kumar, P.K. Priya, H.P. Bhasker, U.B. Singh, R.K. Karn, C. Tyagi, R.P. Yadav. Rad. Phys. Chem., **199**, 110353 (2022). DOI: 10.1016/j.radphyschem.2022.110353

[18] A. Hernandez, Y. Kudriavtsev, C. Salinas-Fuentes, C. Hernandez-Gutierrez, R. Asomoza. Vacuum, **171**, 108976 (2020). DOI: 10.1016/j.vacuum.2019.108976

[19] D. Xia, Y.B. Jiang, J. Notte, D. Runt. Appl. Surf. Sci., **538**, 147922 (2021). DOI: 10.1016/j.apsusc.2020.147922

[20] Y.R. Luo. *Comprehensive Handbook of Chemical Bond Energies* (CRC Press, 2007).

[21] P. Sigmund. *Sputtering by ion bombardment theoretical concepts.* In: *Sputtering by Particle Bombardment I*, ed. by R. Behrisch (Springer Verlag, Berlin, 1981).

[22] H. Gades, H.M. Urbassek. Nucl. Instrum. Meth. B, **88**, 218 (1994). DOI: 10.1016/0168-583X (94)95316-3

[23] M.P. Seah, T.S. Nunney. J. Physica D, **43** (25), 253001 (2010). DOI: 10.1088/0022-3727/43/25/253001

[24] D.R. Lide (ed.). *Handbook of Chemistry and Physics* (CRC Press, 2004).

[25] M. Tanemura, M. Ukita, F. Okuyama. Surf. Sci., **426**, 141 (1999). DOI: 10.1016/S0039-6028(99)00174-0

[26] T. Aoyama, M. Tanemura, F. Okuyama. Appl. Surf. Sci., **100/101**, 351 (1996). DOI: 10.1016/0169-4332(96)00240-1

[27] V.S. Chernysh, A.E. Ieshkin, D.S. Kireev, A.A. Tatarintsev, B.R. Senatulin, E.A. Skryleva. Nucl. Instrum. Meth. B, **554**, 165463 (2024). DOI: 10.1016/j.nimb.2024.165463

[28] M.A. Lively, B. Holybee, M. Toriyama, S. Facsko, J.P. Allain. Sci. Rep., **10**, 8253 (2020). DOI: 10.1038/s41598-020-64971-9

[29] S. Valeri, M. Lolli. Surf. Interf. Anal., **16**, 59 (1990). DOI: 10.1002/sia.740160115

*Translated by J.Savelyeva*